Supplementary Information (SI) for Nanoscale.

Supporting Information:

Nanometrology assisted chemical fabrication: direct laser writing of porphyrins onto complex surfaces

Baptiste Maillot, Haroon Rashid, Roxanne Bercy, Jean Frédéric Audibert, Manuel J. Llansola-Portoles, Isabelle Leray, Fabien Miomandre, Vitor Brasiliense*

S1) Precise determination of molar absorptivity coefficients of TAPP in different solvents

The molar absorption coefficients of TAPP were experimentally determined using UV-visible spectroscopy. To achieve this, a series of solutions was prepared through controlled dilutions from a 7.5 mM parent solution in DMSO, enabling the acquisition of an absorption spectrum for each concentration. The experimental data points were subsequently extrapolated using the Beer-Lambert law to precisely determine the molar absorption coefficient of TAPP. The extrapolation was conducted based on the absorbance values measured at the maximum absorption wavelength of each spectrum (439 nm in DMSO and 428 nm in DCM). This analysis yielded molar absorption coefficients of 70 250 $M^{-1} \cdot cm^{-1}$ (Figure S1A) for TAPP in DMSO and 93 100 $M^{-1} \cdot cm^{-1}$ (Figure S1B) in DCM.

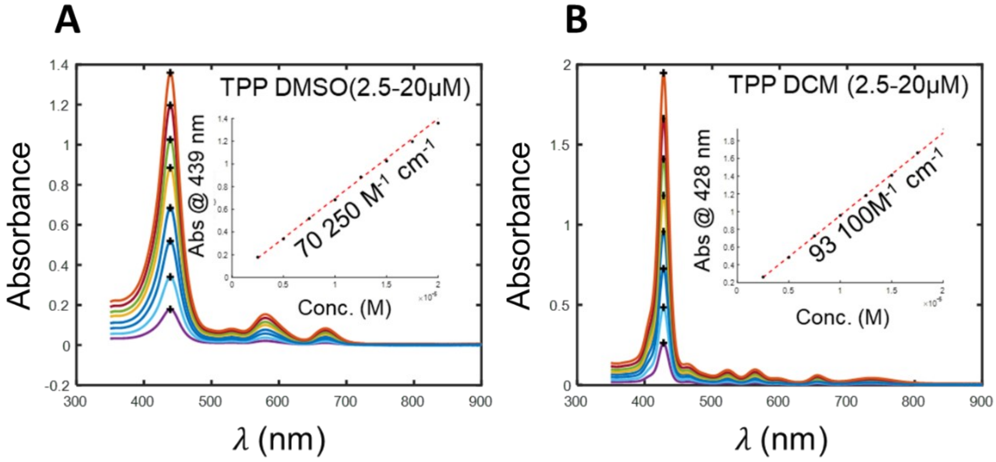

Figure S1. *Determination of molar absorptivity coefficient of TAPP in pure DMSO [A] and pure DCM [B] by UV-visible spectroscopy. The maximal Absorbance is indicated by the '+' signs, and reported in the inset as a function of the Concentration.*

S2) Evolution of UV-visible spectrum of TAPP with the addition of acidic H_2O and organic acid

To investigate the effects of acidic water as a co-solvent on the structure in solution of TAPP, we conducted a titration of this molecule with acidic water (pH = 2, Fig. S2A) and an organic acid (Fig. S2B), monitored via UV-visible spectroscopy. For this study, we selected para-toluene sulfonic acid due to its advantages as a strong acid that is highly soluble in common solvents. The concentrations of water and acid were incrementally increased through controlled additions from parent solutions, and an absorption spectrum was recorded after each addition. In both cases, the addition of an acidic species resulted in a slight blueshift of the band initially observed at 390 nm, along with a significant redshift of the absorption maximum originally at 467 nm. Concurrently, we observed the progressive disappearance of the Q-bands and the emergence of a broad absorption band in the near-infrared region. The comparison of these results indicates that the protonation of the porphyrin ring is responsible for the observed changes in the photophysical properties of the system. At high concentrations of acidic water in the medium (>100 µM), the blueshift of the band initially at 390 nm becomes increasingly pronounced, reaching 427 nm (Figure S2.B). Under these conditions, the structure exhibits two nearly symmetrical absorption bands replacing the initial Soret band maximum.

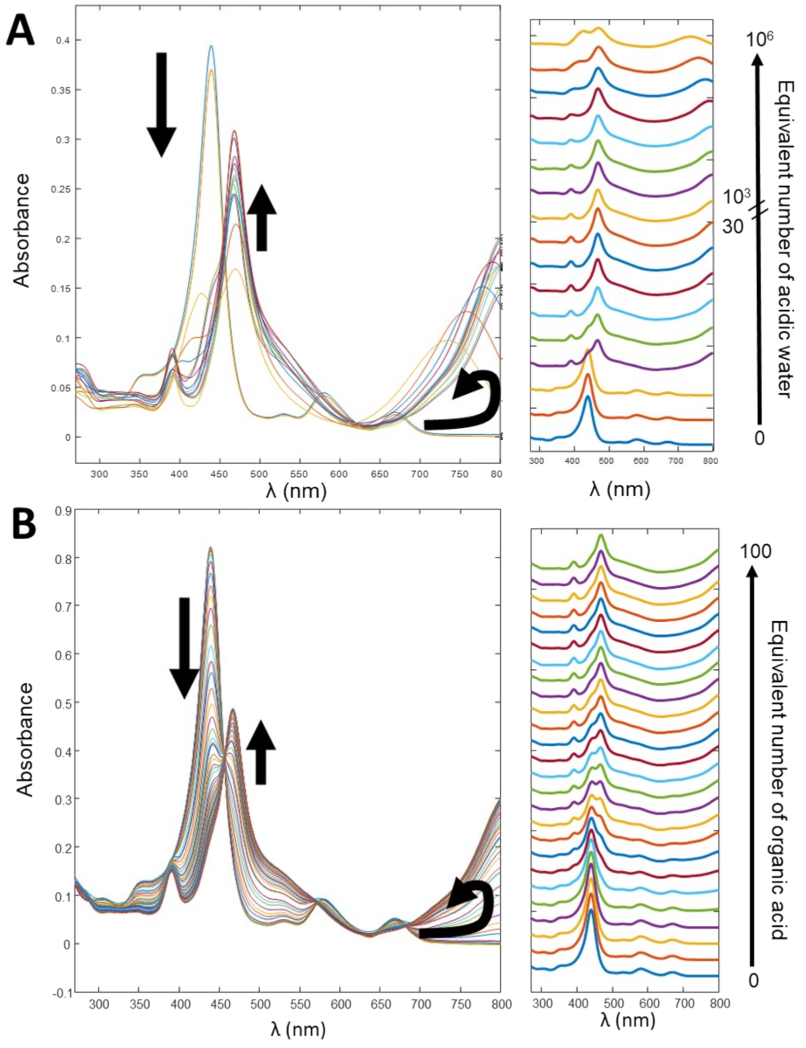

Figure S2. *UV-visible spectrum evolution of TAPP at 10 µM with different equivalent of (A) acidic Milli-Q water and (B) p-toluene sulfonic acid monohydrate. The panels on the right report the same data, vertically displaced to improve readability.*

S3) Fluorescence decay of TAPP in different solvents

Fluorescence lifetime measurements were performed to further characterize TAPP solutions in different solvents. TAPP solutions were excited at 470 nm, and fluorescence emission was collected at the respective emission maxima (DMSO: $\lambda_{exc} =$ 670 nm, DCM: $\lambda_{exc} =$ 650 nm). The fluorescence decay of TAPP in DCM (Figure S3.A) could be fitted with a mono-exponential function, suggesting that TAPP is fully dispersed in this solvent. This observation is in good agreement with the higher molar extinction coefficient measured in DCM (Supporting Information S1). In contrast, the fluorescence decay in DMSO (Figure S3.B) follows a bi-exponential profile, indicating the presence of two distinct populations of emissive molecules. This result suggests that TAPP is not completely dispersed in DMSO but instead exists in an equilibrium between free TAPP molecules and dimers. The fluorescence decay in a 50v% DMSO:H_2O (pH = 2) is more complex (Figure S3.C) and exhibits multi-exponential behaviour. This indicates the presence of several populations of small oligomers in solution, likely consisting of dimers, trimers, etc.

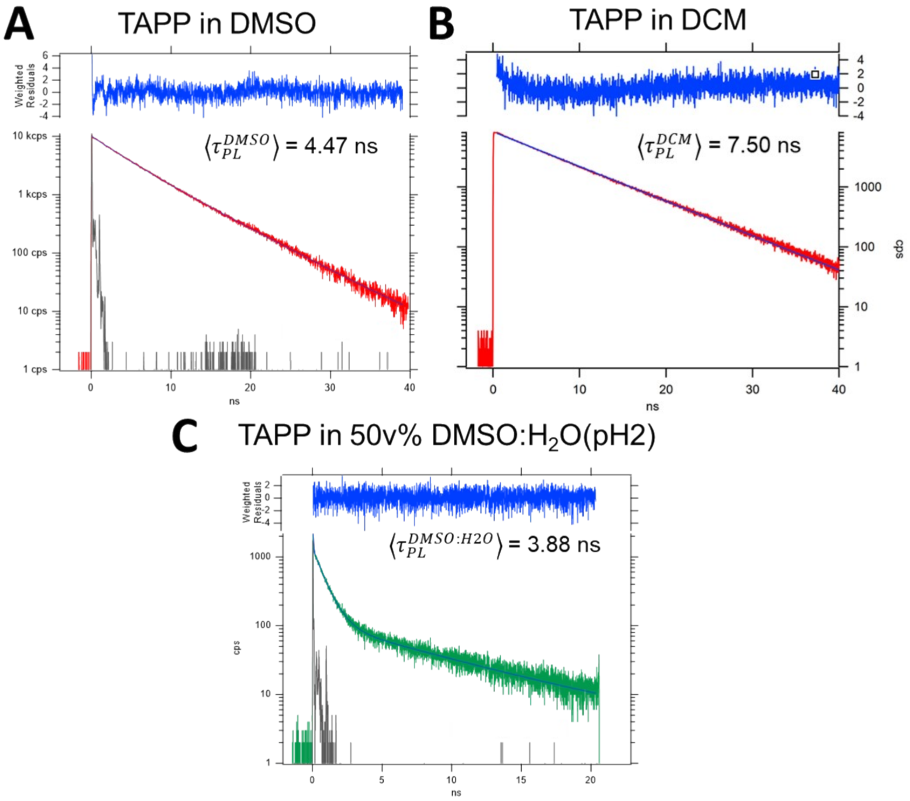

Figure S3. *Fluorescence decay of TAPP at 10 µM in (A) pure DMSO , (B) pure DCM and (C) in a mixture of pH2 water and DMSO (50v%).*

Sample #	a0	τ0 (s)	a1	τ1(s)	a2	τ2	f0	f1	f2	χ^2	Mean Lifetime (s)
DCM	7828	7.5E-9	-	-	-	-	100	-	-	1.257	7.50E-9
DMSO	4139	2.5E-9	5810	6.29E-9	-	-	29	71	-	1.289	4.47E-9
50%v DMSO:H_2O	3891	0.03E-9	1219	0.76E-9	111	7.68E-9	5	49	46	1.220	3.88E-9

Table S1. *Fit parameters used to adjust the curves to exponential models, leading to the fit curves indicated in Fig. S3.*

S4) Resonant Rayleigh spectra of TAPP and Dz TAPP

The results reported in the main text suggest that both DMSO and H_2O are able to solubilize the porphyrin intermediates reasonably well, generating to visibly noticeable precipitation. In this section, we further support this claim, recording Rayleigh light scattering of different solutions.

Rayleigh light scattering spectra are recorded by irradiating a solution and collecting the scattered light at 90^o angle. The excitation and detection wavelengths are controlled by the monochromators, which are set to the same wavelength and simultaneously moved to record the Rayleigh scattering. In this case we collect the diffusion signal of the sample at each wavelength. The presence of peaks in the spectrum indicates the presence of aggregates in solution which diffuse the incident light sent on the sample.

No significant peak is observed in 50v%H_2O for either TAPP or Dz TAPP, as indicated below (Figure S4). This suggest that porphyrin derivatives are at least reasonably well solubilized in this solvent, as extensive aggregation is not observed.

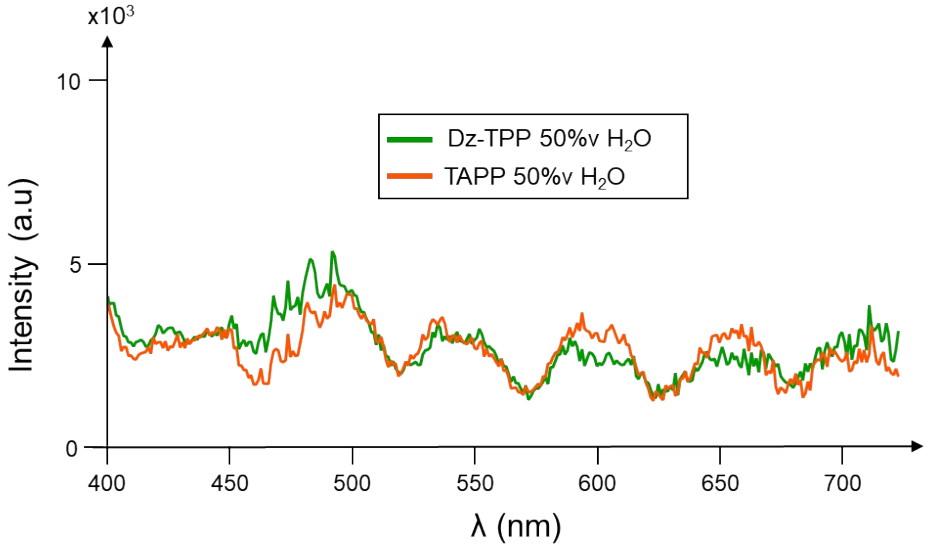

Figure S4. *Rayleigh light scattering spectra of TAPP (in green) and Dz-TPP (in orange) in a mixture of pH2 water and DMSO (50v%).*

S5) Spectroscopic characterization of TAPP Dz structure in solution

The molar absorption coefficient of Dz TPP was determined using UV-visible spectroscopy following the method described in S1. Extrapolation with the Beer-Lambert law at the absorption maximum (458 nm) yielded a molar extinction coefficient of 95500 $M^{-1}\cdot cm^{-1}$ (Figure S5.A). This value is very similar to that found for TAPP in DCM, suggesting that the structures of the two species in these media are identical. Consequently, it can be inferred that Dz TAPP is present in a dispersed form in acidic aqueous solution. To further investigate, a more detailed photophysical study was conducted by varying the proportion of DMSO in the medium. A 5 mM parent solution of Dz TPP was prepared in a 50 : 50 H_2O (pH = 2) : DMSO mixture. After 2 hours of reaction, this solution was diluted to 10 µM in mixtures with varying proportions of H_2O (pH = 2) and DMSO. The results, shown in Figure S5.B, indicate that the excitation spectra closely resemble the absorption spectra, suggesting that water in the mixture enables dispersion of the cationic species formed after diazotization. These results clearly demonstrate that Dz TAPP is predominantly in a monomeric form in solution.

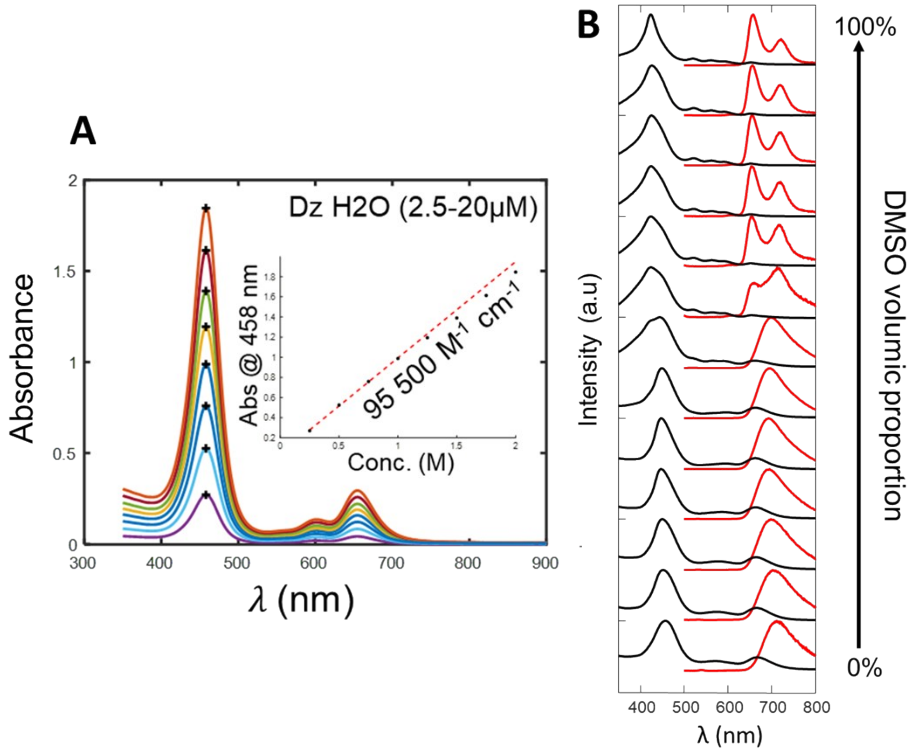

Figure S5. *Determination of molar absorptivity coefficient of TAPP Dz in pure water (pH=2) [A] Excitation (black) and emission (red) spectra evolution of TAPP Dz at 10µM in different proportion of DMSO:H2O (pH=2) [B]*

S6) Effect of laser power on Dz TAPP grafting efficiency

Photografting experiments were performed to measure the grafting efficiency (η_{app}) of Dz TAPP. This efficiency is defined as the ratio of the deposition rate on the surface to the incident power delivered to the sample. It was first observed that adding a photosensitizer, such as rhodamine 6G in an equimolar proportion, increased the grafting efficiency(Figure S6). This demonstrates that the photografting reaction efficiency can be significantly increased through use of a sensitizer. Additionally, as the incident laser power is increased, a decrease in the apparent grafting efficiency is observed, consistently with a diffusion limited reaction rate.

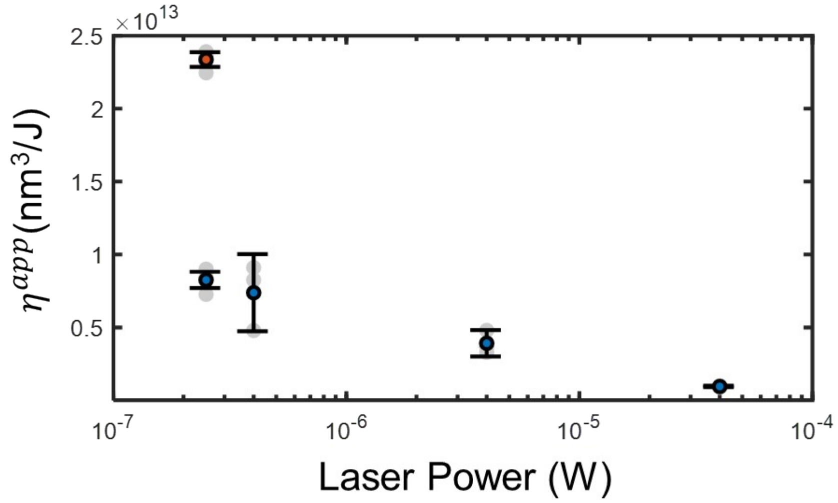

Figure S6. *Evolution of the grafting efficiency of 5mM Dz- TAPP solution at different laser power (*λ_{exc} *= 474 nm) in absence (blue) and in presence (orange) of sensitizer.*

S7) AFM measurements of grafted TAPP

Atomic Force Microscopy ex situ measurements of several repetitions of the controlled photografting experiment, enabling characterization of the precision of the controlled grafting operation. The grafting operation was realized in 5mM 50 v% DMSO:H_2O (pH=2) solution of TPP Dz. The process was controlled using adaptative algorithm method (described in detail elsewhere[1]) with a target optical volume difference of 10^7 nm^3, with a 250 nW (1.25 mW/cm^2) laser power and initial illumination interval of 1s.

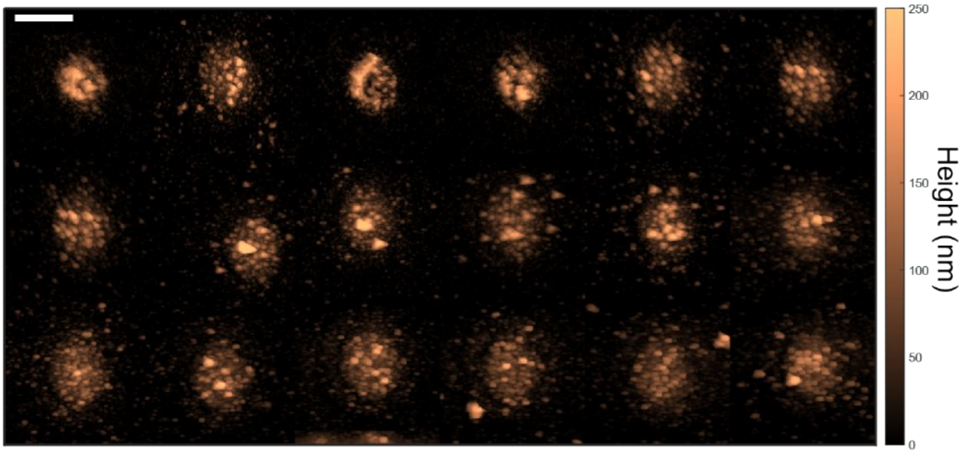

Figure S7. *Atomic force microscopy (AFM) images showing typical results of single point grafting operations of Dz-TPP, controlled in situ with the help of nanometrology based control. The scale bar represents 2 µm.*

Reference:

[1] B. Maillot, J. F. Audibert, F. Miomandre and V. Brasiliense, Nanoscale, 2024, 16, 7594–7602

S8) Optimization of Sensitizer to diazonium ratio with 4-Nitrobenzenediazonium

The ratio of grafting entity to sensitizer was optimized by analyzing the evolution of the grafting rate with time at different concentrations of R6G sensitizers, at a constant laser power of 1.5µW.

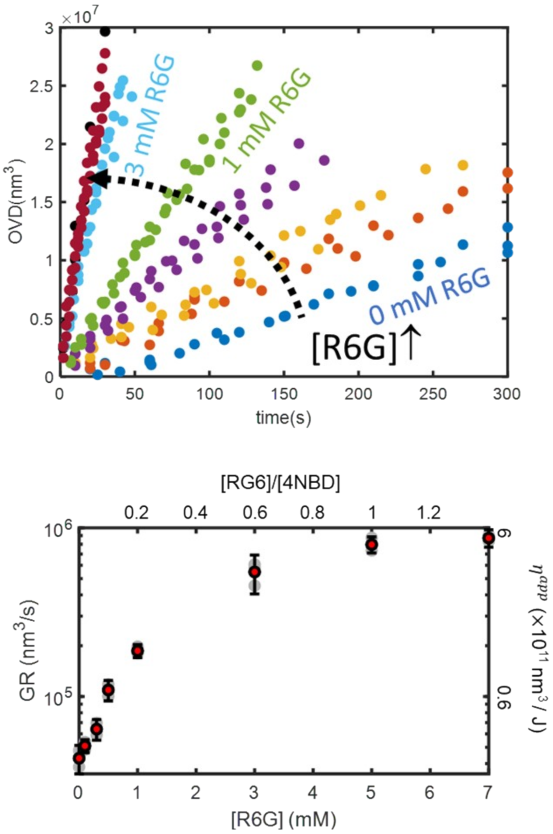

Figure S8. Optimization of the ratio between 4-nitrobenzenediazonium grafting molecule and R6G sensitizer. Quantitative Phase Imaging monitoring of the evolution of the optical volume of the grafted layer by irradiating (1.5 µW) 5mM 4NBD aqueous solutions in the presence of different concentrations of R6G sensitizer. The slopes of the curves are used to estimate a Grafting Rate (GR), or apparent efficiency (η^{app}), reported in the bottom panel.

S9) Analysis of the Chemical properties of the grafted layers

The surface chemical properties of the grafted layer are characterized *ex-situ* through a combination of Vibrational (Raman) spectroscopy and X-ray surface analysis, described here. First, Raman spectroscopy is used to demonstrate the presence of porphyrin moieties in the grafted layer, confirming that the photochemical modification process does not disrupt the TPP structures. Then, we use EDS/SEM analysis to provide a first estimation of the chemical composition of the layer, comparing grafted areas with background (non irradiated) zones. This preliminary analysis is completed by high resolution XPS spectra of the grafted zone.

S9.1) Raman Spectrum of the grafted layers

Raman spectra are recorded on the “ENS Paris-Saclay” sample, as described in the main text. All vibrational modes observed in the Raman spectrum of the grafted layer (Figure 3 in the main text), can be satisfactorily assigned to well defined normal modes, as reported in the table below. We compare the observation band positions with literature data, supporting the assignments. Normal modes are reported according to its the dominant internal coordinate, following the methodology of [3]. While small differences can be occasionally observed, especially for modes which are weak (847 cm^{-1}, and 1141 cm^{-1}) or poorly resolved (as in the 1290-1550 cm^{-1} region), we observe excellent agreement between the modes measured in the layers and reported data.

Band obs $\pm$10cm^{-1}	Rel. Int.	Assignement	Reported data (cm-1)	Δ (cm^{-1})
847	vW	δ_s(ring(X))	[3]833	[3]14
887	W	δ_s(ring(N))	[3] 886	[3]1
967	M	$\nu(C_aC_m)$	[1]983(w), [2]963, [3]962	[1]16, [2] 4, [3]5
1006	M	$\nu(C_a\text{-}H)$	[1]1012,[1’] 1004 -1011, [2]1003, [3]1004	[1]6, [1’] 2-5, [2] 3, [3]2
1078	W	$\nu(C_bH)$	[1]1078, [1’] 1079 [2] NR, [3]1076	[1] 0, [1’] 1, [2]NR, [3]2
1141	Vw	$\nu(C_aN)$	[1]1183, [3]1135	[1]42, [3]6
1238	S	$\nu(C_m\text{-}Ph)$	[1]1247,[1’] 1237, ν_1 [2]1238, [3] 1234	[1] 9, [1’]0, [2] 0, [3]4
1293	S	$\nu(C_aC_b)$	[1]1289(w),[1’] 1286(w), [2]1296, [3]1292	[1]4,[1’] 7,[2] 3, [3]1
1322	M	-	[1]1324 [1’] 1329 [2] NA,[3] NA.	[1]2, [1’] 7,[2] NA, [3]5
1360	M	ν(Ca-N(N))	[1]1366 [1’]1365 [2]1362(w) [3]1357	[1]6, [1’]5, [2]2, [3]3
1444	M	$\nu_{as}(C_aC_m)$	[1]1470, [1’] 1476 [2]1465(w) [3] 1438	[1]26, [1’] 32, [2] 21, [3]4
1553	S	$\nu(C_bC_b(N))$	[1]1532, ν_2 , [1’] 1544, [2]1555 [3] 1550	[1]19, [1’] 9,[2] 2, [3]3
1599	m	[3] Phenyl Mode	[1]1598 [1’] 1598,[2]1600, [3] 1597	[1] 1, [1’] 1, [2]1, [3]1

Table S2. Comparative analysis of the vibrational bands observed in the Raman spectrum of the grafted layer, including the mean position, relative intensity, tentative assignment (based on the modes described in [3]), direct comparison with the data reported for solutions of free base tetraphenyl porphyrins: [1] TAPP in trifluoroacetic acid (TFA), [1’] TPP in TFA, [2] TPP in Tétrahydrofuran, and [3] TPP in benzene. Differences between the frequencies observed in our layer and literature data are reported in the Δ column.

S9.2) SEM/EDS Data

As SEM analysis requires the samples to be conductive, a sacrificial sample was used to study elemental distribution within the sample. A pattern consisting of a 20x20 grid is prepared from a 5mM Dz-TPP solution in DMSO:H2O, as described in the main text for the "ENS Paris-Saclay" sample, which is subsequently sputtered with gold (thickness 7±3 nm). SEM images of the grid are shown in Fig. S9-2a. EDS analysis is performed on the grafted zone (Fig.S9-2b) and in the background (Fig.S9-2c), resulting in the EDS spectra shown in Fig.S9-2d. Elemental identification of the different peaks is performed automatically using the Team software (eZAF Smart Quant), yielding the peak identification indicated in the figure. Mean results are summarized in Table S9-3, along with statistics based on a large number of repetitions (N=17) of the experiment for slightly different spots within the same zone. No evidence of spontaneous adsorption or grafting is observed. Indeed, while background areas (ca. 20-30 µm to the left of the pattern) only show peaks associated with the presence of Na, Al, Si, O and Au (all present in the coverslip borosilicate composition), C and N peaks are only present in the irradiated zones. These results show that any C or N surface content require irradiation.

Element	***Weight%***	***Atomic%***
C K	*43.0 ± 1.5*	*57.6 ± 1.6*
N K	*5.3 ± 0.3*	*6.0 ± 0.3*
O K	*24.4 ± 0.9*	*24.7 ± 1.0*
Na K	*3.8 ± 0.3*	*2.7 ± 0.2*
Al K	*1.9 ± 0.5*	*1.1 ± 0.25*
Si K	*13.23 ± 0.9*	*7.0 ± 0.8*
Au M	*9.5 ± 0.9*	*0.8 ± 0.1*

Table S3. Summary of the EDS analysis after fit of the data (eZAF Smar Quant) in the grafted zone. The mean values of N=17 measurements are indicated, collected at the spots indicated in Fig.S9-2B, along with 3σ error.

It is also interesting to analyse the ratio between the N and C atomic% (henceforth called the N/C ratio) in the grafted zone, revealing an average value of 0.104 ± 0.015 (3σ error, based on N=17 measurements). If all N and C contents are assigned to TPP molecules, this value indicates an average of 4.6 ± 0.6 atoms of C per porphyrin. This is consistent with the 4 to 44 N to C proportion expected from TPPs, albeit a bit higher than expected. Excess N can be readily explained by the presence of azo bridges, often observed during diazonium-based grafting operations[4,5]. In contrast, no C or N are detected on non -irradiated zones, therefore indicating that no spontaneous adsorption takes place and showing that C and N content of the sample are coming from the irradiated zone.

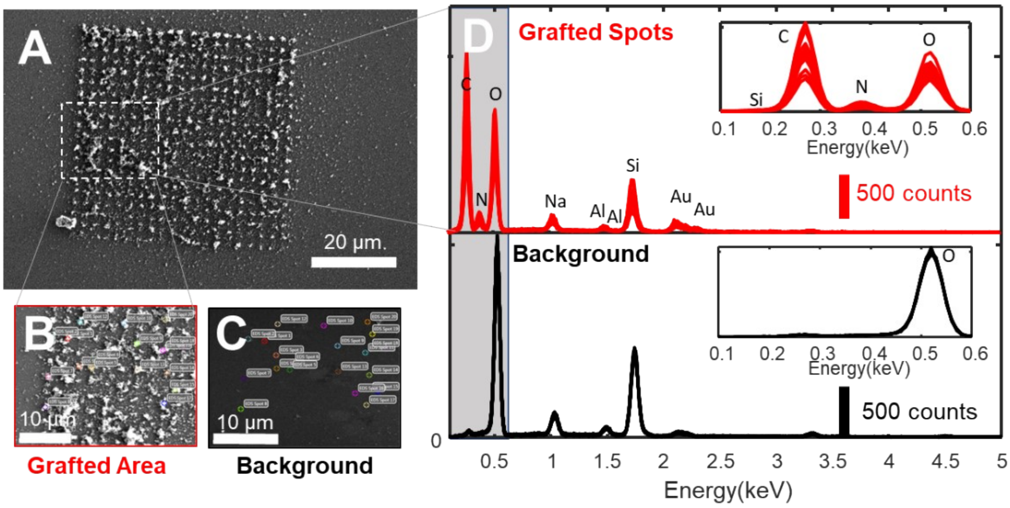

Grafted Area **Background**

Figure S9-2. SEM/EDX analysis of a 20x20 grid sample, obtained by sequentially grafting 400 TPP spots and depositing a thin Au layer to increase the surface conductivity. (A) Global SEM image of the pattern. (B) Zoom into the zone analyzed with EDX, and (C) into the background area (~ 30µm away from the grafted pattern). The resulting EDX spectra are shown in (D), showcasing the presence of C and N signals, which are practically absent in the background zone.

S9.3) X ray Photoelectron spectroscopy Data

The previous SEM/EDS analysis are further complemented by detailed XPS study of the “ENS Paris-Saclay” sample (Fig.3 of the main text). XPS data is collected using a 400 µm beam focused on the grafted zone, leading to the spectra shown in Fig. S9-4a-c. Since the layer is prepared on SiO_2 coverslip, it is difficult to extract information from Silicon or Oxygen regions, therefore we rely on the analysis of C and N regions, whose fit is shown in Table S9-5. The C 1s carbon region is shown in S9-4b, and indicates the presence of three components, at 284.7 (accounting for 72% of the total C content), 286.1 (16%) and 288.2 eV (12%). The main component is assigned to porphyrin carbons connected to other carbons, or hydrogen (C-C/C-H), while higher energy binding energies are associated to carbons connected to more electronegative elements. We assign the 286.1 eV peak to C-N=C bonds from the porphyrin structure, due to comparison with literature, and due to the atomic proportion of such carbons of 16%, which is in reasonable agreement with the expected proportion of 18% for TPPs. The 288.2 eV peak is associated to the presence of C=O bonds [7], which can correspond to either adsorbed CO_2 from the environment, or to oxidation species which are likely to form during excitation of the porphyrins in the presence of oxygen due to formation of singlet oxygen (during collection of the fluorescence and FLIM images). Figure S9-4c shows the analysis of the N 1s region of the spectrum, dominated by a single peak centred at 399.98 eV, representing 93% of the N content of the sample. Two much smaller contributions can be found at 402.57 eV (2% of the N content) and 405.81 eV (5% of the N content). The main peak position is consistent with both the nitrogens from the porphyrin main cycle (typ. at 400.2 eV[6]), and with the presence of diazo bridges (typ. at 400 eV [4,5]), therefore

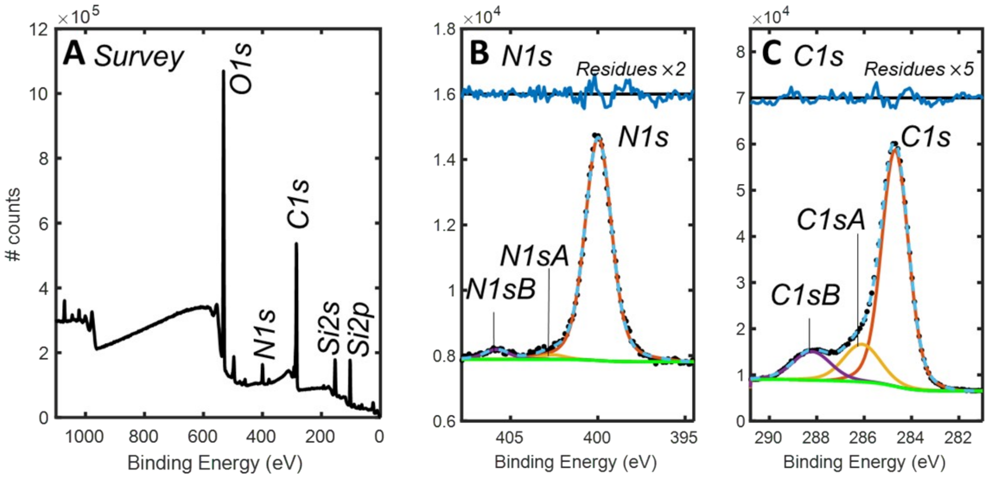

Figure S9-4 XPS spectra of the "ENS Paris-Saclay" sample, shown in Fig.3 of the main text. (A) survey analysis of the XPS sample. (B) Detailed XPS spectra of the C 1s region arount 285 eV, (C) detailed XPS spectrum collected at the N 1s region, around 400eV. Experimental points are shown as black dots, baseline corrections are shown in green, fit data is shown as full lines, and the final fit

Name	Peak BE	FWHM eV	Area (P) CPS,eV	element atomic %	Total Atomic %
C1s	284,69	1,34	76498,53	72	31,18
C1s A	286,1	1,83	16656,87	16	6,79
C1s B	288,21	1,89	13075,94	12	5,34
C total				100	43,31
N1s	399,98	1,8	14249,13	94	3,74
N1s A	402,57	1,72	293,94	2	0,08
N1s B	405,81	1,72	630,16	4	0,17
N total				100	3,99

Table S4 Summary of the fitting analysis of the XPS spectra.

we rely on elementary analysis and N/C ratios to differentiate between the two. We assume that all C and N are coming from the grafted patterns, which is a reasonable on the account of our previous EDS study, which revealed no significant C or N contribution from background zones. Accounting for all N and C contributions, a N/C ratio of 0.092 ± 0.01 is obtained, indicating a 4.0 ± 0.4 N per porphyrin, consistently with our previous EDS estimations, Raman and photoluminescence spectra, therefore confirming the layer is majorly formed of TPPs.

References:

[1] I. H. Wasbotten, J. Conradie and A. Ghosh, J.Phys.Chem.B, 2003, 107, 3613–3623.
[2] S. E. J. Bell, A. H. R. Al-Obaidi, M. J. N. Hegarty, J. J. Mcgarvey and R. E. Hester, J. Phys. Chem, 1995, 99, 3959–3964.
[3] P. Stein, A. Ulman and T. G. Spiro, J. Phys. Chem, 1984, 88, 369–374.
[4] P. Doppelt,G.Hallais, J.Pinson, F. Podvorica, S. Verneyre Chem. Mater. 2007, 19, 4570-4575.
[5] R. Ahmad, L.Boubekeur-Lecaque, M. Nguyen,S. Lau-Truong, A.Lamouri,P. Decorse, A.Galtayries, J.Pinson,N.Felidj,C.Mangeney J. Phys. Chem. C 2014, 118, 19098−19105
[6] P. Macquet, M. Millard, T. Theophanides J. Am. Chem. Soc. 1978, 100,15, 4741-4746.
[7] Beamson G, Briggs D. High Resolution XPS of Organic Polymers – The Scienta ESCA 300 Database. John Wiley & Sons: Chichester, 1992.

S10) Influence of sensitizer on emission spectra of grafted layers

The influence of the sensitizer on the grafted layer properties was analyzed by photografting porpyrin based layers in in the presence and absence of sensitizer. The local emission spectrum of each layer is recorded by exciting the layers with a (r_{beam} = 400 nm) in using the 474 nm laser source. As clearly visible in Figure S10, both polymers layer exhibits the same photophysical properties, which display the two characteristic bands associated to TPP layers (at 670 and 720 nm). No trace of rhodamine 6G emission was observed (expected at λ_{max} = 550 nm), demonstrating that the photosensitizer contribution to the grafted layer is negligible.

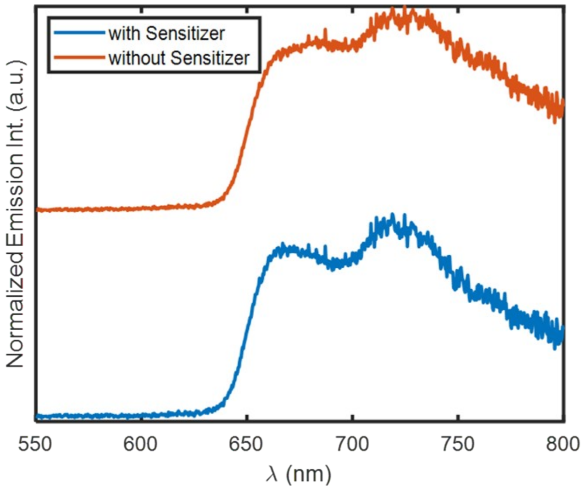

Figure S10. *Emission spectrum of TAPP grafted layer with (in blue) and without (in orange) the use of rhodamine 6G as a photosensitizer in the grafting solution*

S11) Grafted Layers lifetime analysis and FLIM data treatment

Fluorescence decay FLIM data were fit to a discrete multiexponential function, containing four (N=4) terms, as indicated below. The curves are normalized with respect to the number of pixels used in the analysis.

$$y = \sum_{i=0}^{N} a_i e^{-\frac{t}{\tau_i}}$$

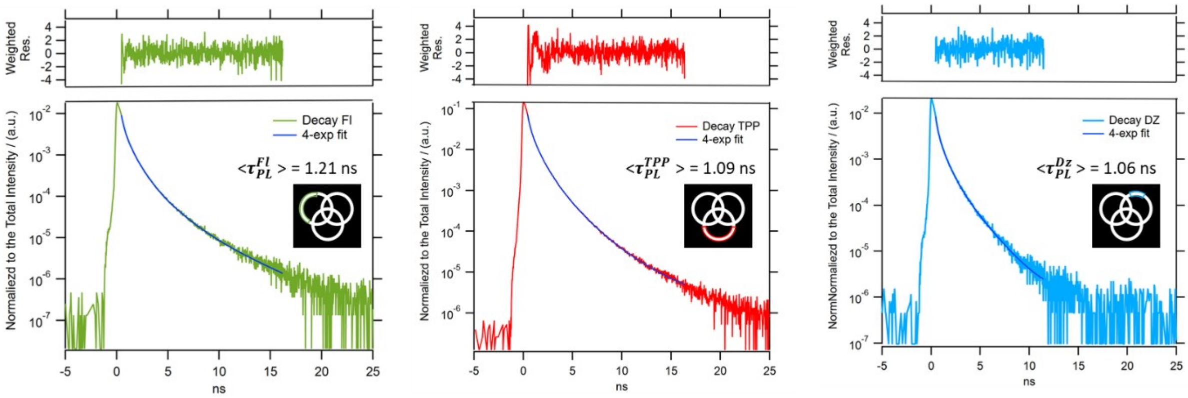

Figure S11. *Fluorescence decays of Fl (green), TPP (red) and DZ (blue) adjusted by a 4-exponential model (deep blue). For each sample signal is extracted from the corresponding region of interest (inset).*

Sample #	**ROI area in pxl**	**Total intensity in photon**	**Photon/pxl/s**
Fl	2855	4.83E+06	0.2
TPP	2405	3.26E+07	4.3
DZ	893	1.54E+06	0.5

Sample #	**a0**	**τ0**	**a1**	**τ_1**	**a_2**	**τ_2**	**a_3**	**τ_3**	**χ^2**	**f0**	**f1**	**f2**	**f3**	**Mean lifetime**
Fl	4.10E+04	2.33E-10	33034.5	**7.11E-10**	7443.74	**1.64E-09**	566.112	**4.06E-09**	1.37437	20.09	**49.39**	**25.69**	**4.83**	1.21E-09
TPP	2.74E+05	2.40E-10	211130	**6.85E-10**	59293.7	**1.46E-09**	3878.29	**3.16E-09**	1.55339	21.31	**46.75**	**27.98**	**3.96**	1.09E-09
DZ	12030.4	2.04E-10	918328	**6.34E-10**	1556.47	**1.26E-09**	1290.64	**1.87E-09**	1.1737	19.41	**46.6**	**15.47**	**19.06**	1.05E-09

Table S5. *(top) Reported values of the corresponding region of interest for each sample. (bottom) Fits results of the adjustment by a 4-exponential model. The intensity mean lifetime is calculated considering the 3 last contributions only. The first fractional intensity contribution f_0 with a short life time is mainly attributed to the scattering of the excitation.*

S12) Synthesis of fluorescein azide derivative (Az-Fl) and Click reaction

Synthesis of the Fluorescein azide derivative. Azide functionalized fluorescein was synthetized in 2 steps without purification, following a protocol adapted from [1]. In a 1 mM s50%v DMSO :milli-Q water solution of fluorescein-p-amine, we add 9 equivalents of para-toluenesulfonic acid monohydrate and 9 equivalents of $NaNO_2$, forming the diazonium fluorescein derivative. After 1 hour, 1.6 equivalents of sodium azide are added, leading to the desired fluorescein azide derivative in about 5 minutes. All steps are carried out at room temperature.

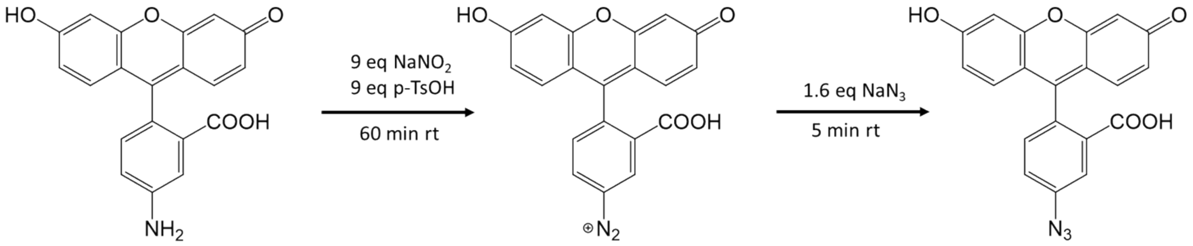

Figure S12. *Scheme indicating the different steps of the fluorescein azide derivative synthesis*

Post-functionalization of the alkyne layer with fluorescein. A postfunctionalisation “click” solution is freshly by dissolving 1mM Fluorescein-azide, 1mol% Cu(II) acetate and 2mol% Sodium L-ascorbate in 50v% H2O:DMSO, degassed (N_2) for ca. 5 min. The surface containing the alkyne-terminated grafted layers (prepared from 5mM alkyne diazonium as described in the main text) is immersed in the “click” solution and left to react at room temperature for about 12 hrs, leading to functionalization with the fluorescent moiety. The sample is carefully rinsed with milli-Q water after each step.

Reference:

[1] K. V. Kutonova, M. E. Trusova, P. S. Postnikov, V. D. Filimonov, J. Parello, Synthesis, 2013, 45, 2706-2710

S13) Photophysical properties of polymer layers functionalized by fluorescein derivative

The photografted polymer grid is prepared in our homemade setup in using a 5mM solution of alkyne diazonium. The piezoelectric system described in the main text is used to control the grafting spot, forming a regular grid of 30 x 30 spots with 3µm spacing. Each spot is illuminated with the laser beam ($\lambda_{exc} =$ 474 nm) for 250 ms.

After the photografting procedure, we confirm the success of the operation by acquiring a microscope transmission image (Fig13A), imaged at λ_{obs}=633 nm to avoid formation of radicals. After post functionalizing the grid using the procedure described in Section S12 and abundant rinsing with water, the photophysical properties of the layer are analyzed by fluorescence spectroscopy (Fig.13B). For that, the emission spectrum of the functionalized layer is excited at $\lambda_{exc} =$ 474 nm, in a widefield illumination (r_{col} = 20µm) configuration. An 520 nm excitation filter is used to reject the excitation wavelength and record the emitted photons (integration time : 1s). We compare the resulting emission spectrum of the fluorescein azide derivative solution (Figure S12.B), recorded in a cuvette at 470 nm excitation with a Fluorolog. Excellent agreement is observed between the two spectra, confirming the functionalization of the grid with fluorescein derivatives.

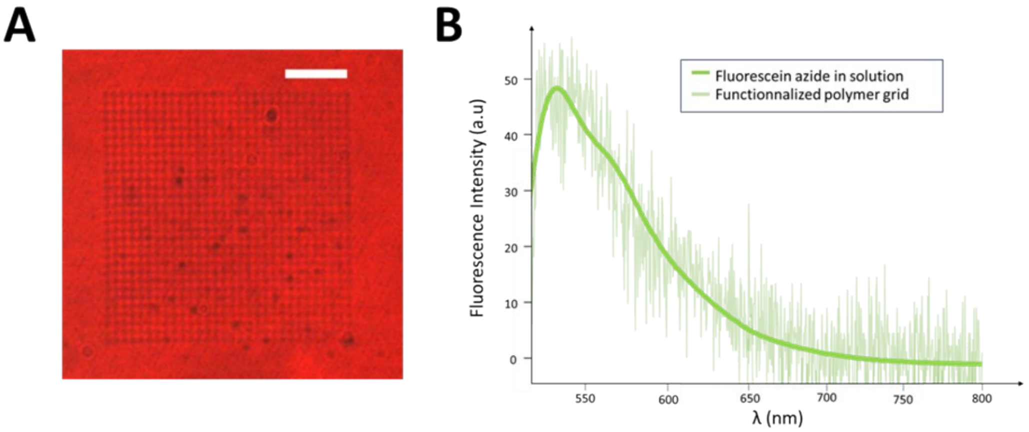

Figure S13. *Transmission image (λ_{obs} = 633nm) of the photografted alkyne polymer grid. The scale bar represents 22.5 µm (A). Comparison between the emission spectra of the functionalized polymer grid and the fluorescein derivative in solution [B].*